LOW-MASS STAR FORMATION: THEORY

FRANK H. SHU, ANTHONY ALLEN, HSIEN SHANG,
Astronomy Department, University of California
Berkeley, CA 94720-3411, USA
EVE C. OSTRIKER
Astronomy Department, University of Maryland
College Park, MD 20742-2421, USA
AND
ZHI-YUN LI
Department of Astronomy, University of Virginia
Charlottesville, VA 22903, USA

1. Magnetic Support of Clouds

Molecular clouds, the cradles of star birth, are supported against self-gravity in part by magnetic fields (McKee, this volume). In 1956, Mestel & Spitzer (see also Mestel 1965) introduced a mass scale associated with the amount of magnetic flux Φ threaded by a self-gravitating, electrically conducting, cloud. This scale, the magnetic critical mass,

$$M_\Phi \equiv \frac{\Phi}{2\pi G^{1/2}}, \tag{1}$$

is potentially as important for our subject as the Chandrasekhar limit is for the theory of stellar evolution (see Chandrasekhar 1939 and Schwarzschild 1958). In equation (1), G is the universal gravitational constant, and the rest of the equation differs from Mestel & Spitzer's (1956) definition (see also Mouschovias & Spitzer 1976) only by the value of the numerical coefficient on the right-hand side. Our choice of the numerical coefficient $1/2\pi$ defines M_Φ to be the maximum mass that can be supported if the magnetic field acted alone to oppose the self-gravity of the cloud, so that the cloud becomes highly flattened (see below).

Consider the mechanical equilibrium of a static cloud of mass M and constant temperature T, which occupies volume V (not necessarily spherical or highly flattened) and has a magnetic flux Φ frozen into it while it is being subjected to a slowly changing external pressure $P_{\rm ext}$. The virial theorem applied to such a gas cloud yields (Strittmatter 1966; see also Chapter 24 of Shu 1992)

$$P_{\rm ext} = \frac{a^2 M}{V} + \frac{\alpha G}{V^{4/3}} \left(M_\Phi^2 - M^2 \right), \tag{2}$$

where $a \equiv (kT/m)^{1/2}$ is the isothermal sound speed (with k being Boltzmann's constant and m being the mean molecular mass of the gas) and α is a positive numerical coefficient of order unity. The first term on the right-hand-side of equation (2) is the contribution from Boyle's law, $P_{\rm ext} = NkT/V$ where $N \equiv M/m$, whereas the second and third terms, proportional respectively to $GM_\Phi^2/V^{4/3}$ and $GM^2/V^{4/3}$, yield the corrections associated with magnetic forces and self-gravity. Notice that the latter two forces, expressed per unit area, scale with V in the same way, as $V^{-4/3}$. Thus, on average magnetic forces act effectively to dilute self-gravity (if $M_\Phi < M$) or to reverse it (if $M_\Phi > M$). This property of magnetic forces has profound implications for the problems of gravitational collapse and fragmentation of molecular clouds. These implications can potentially nullify conclusions which are drawn from calculations that ignore its presence.

Figure 1 shows a plot of $P_{\rm ext}$ versus V in the two cases: $M > M_\Phi$ and $M < M_\Phi$. In either case, a cloud of large volume V compresses at first under increases of external pressure according to Boyle, because at large V the average internal thermal pressure $a^2 M/V$ is more important in balancing the external pressure than either magnetic forces or self-gravity. The situation changes dramatically at small V, where magnetic forces and self-gravity both increase more rapidly, but in opposite directions, than the internal thermal pressure.

When the cloud is *magnetically supercritical*, $M > M_\Phi$, the net force from magnetic fields and self-gravity is attractive, and less external pressure is needed to achieve a given decrease in the cloud volume than predicted by an extrapolation of Boyle's law to small V. In particular, if the external pressure increases beyond the maximum value $P_{\rm max}$, the cloud can be pushed over to gravitational collapse.

When the cloud is *magnetically subcritical*, $M < M_\Phi$, the net force from magnetic fields and self-gravity in equation (2) is repulsive, and more external pressure is needed to achieve a given decrease in the cloud volume than predicted by an extrapolation of Boyle's law to small V. In particular, the external pressure required to compactify the cloud increases without bound as V approaches zero. In this case, no amount of external compression can induce the cloud to collapse. Frozen-in magnetic flux will resist the transformation of molecular clouds to stars when the cloud mass M is less than the magnetic critical mass M_Φ as much as electron degeneracy

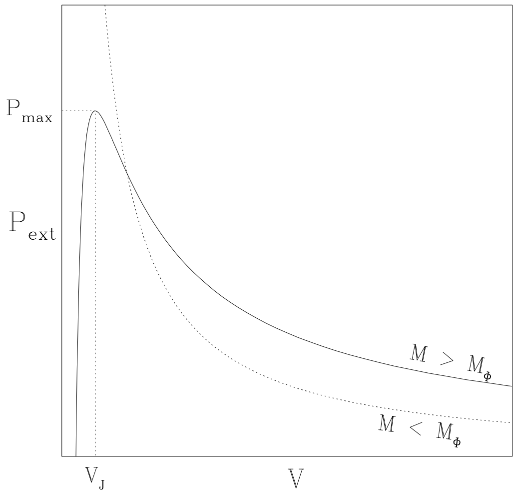

Figure 1. The external pressure $P_{\rm ext}$ needed to compress a magnetized, self-gravitating, molecular cloud to given volume V as estimated by the virial theorem. The two curves for the magnetically supercritical case, $M > M_\Phi$ and the magnetically subcritical case, $M < M_\Phi$ are computed for the same M_Φ, but different M.

pressure will resist the transformation of a white dwarf to a neutron star when the white dwarf's mass is less than the Chandrasekhar limit.

2. Fragmentation

For a magnetically supercritical cloud, it is a simple exercise to show from equation (2) that the condition $P_{\rm ext} = P_{\rm max}$ is reached at a volume $V = V_{\rm J}$ that satisfies

$$V_{\rm J}^{1/3} = \frac{4\alpha GM}{3a^2}\left[1 - \left(\frac{M_\Phi}{M}\right)^2\right]. \tag{3}$$

Apart from the modification factor, $[1 - (M_\Phi/M)^2]$, which has a value between 0 and 1 when $M > M_\Phi$, the length scale $V_{\rm J}^{1/3}$ is defined so that the (negative of the) associated gravitational energy per unit mass $3\alpha GM/V_J^{1/3}$ equals 3/2 of the thermal energy per unit mass, $3a^2/2$. Thus, equation (3) yields the (modified) Jeans criterion [see also Ebert (1955) and Bonnor (1956)]: A cloud of mass M and temperature T will collapse gravitationally if it is compressed to an average size less than the (magnetically modified) Jeans length $V_{\rm J}^{1/3}$.

In the absence of magnetic fields, the Jeans mass $\propto G^{-3/2}a^3\langle\rho\rangle^{-1/2}$ in isothermal collapse decreases as the mean density $\langle\rho\rangle$ increases upon contraction. This behavior underlies Hoyle's (1953) conjecture that a collapsing isothermal cloud will undergo hierarchical fragmention [but see the differing opinions expressed by Hunter (1962), Layzer (1964), Bodenheimer (1980), Tohline (1982), and Boss (1999)]. In the presence of frozen-in magnetic fields, where Φ remains fixed to the collapsing M, notice that the critical mass M_Φ is unaltered by contraction, completely unlike the behavior of the Jeans mass. Thus, for unstable clouds that collapse from initial states not too far removed from being critically magnetized, Mestel & Spitzer (1956) speculated that fragmentation would be suppressed by the presence of frozen-in fields. Mestel (1965, 1985) later surmised that supercritical clouds which flatten dramatically during the collapse might fragment. We shall reexamine this question in §7.

For a magnetically subcritical cloud, no upper limit exists to the external pressure that the cloud can withstand without undergoing continued gravitational contraction. In these circumstances, neither a physically relevant Jeans length nor a physically meaningful Jeans mass can be defined.

3. Empirical Measurements of the Mass-to-Flux Ratio

Given the dichotomy offered by the two choices, $M < M_\Phi$ and $M > M_\Phi$, it is clearly an important matter to measure the mass-to-flux ratio, M/Φ, in actual clouds and compare it to the critical ratio $(2\pi G^{1/2})^{-1}$ (i.e., to measure the dimensionless ratio M/M_Φ). Crutcher (1999, see also Crutcher et al. 1993) has compiled all the reliable Zeeman measurements of the magnetic field strength made to date in molecular clouds. In Table 1, we reproduce the important portion of his summary of the observational data.

In the first column, we have the region measured; in the second column, the inferred column density of molecular hydrogen, $N(\mathrm{H}_2)$; in the third column, the measured strength of the magnetic field along the line of sight, $B_{||}$. In the fourth column we assume a mean molecular mass $m = 2.4\, m_H$, where m_H is the mass of the hydrogen atom; and we ratio the (projected) mass per unit area, $mN(\mathrm{H}_2)$, to the (projected) flux per unit area, $B_{||}$, expressing the ratio in units of $(2\pi G^{1/2})^{-1}$. The fourth column has values that are typically 2 to 5. Nominally, these molecular clouds are magnetically supercritical, which is the conclusion arrived at by Crutcher, who used slightly different formulae. But as Crutcher also noted, there are two systematic effects for which we may need to apply corrections.

First, the total field strength, B, is on average *twice* as large as a component of it, $B_{||}$, seen along some random direction. Second, if molecular clouds are highly flattened (as in the toy model in §7), then a measurement

TABLE 1. Zeeman Measurements from Crutcher (1999)

Cloud	$N(\mathrm{H}_2)$ (10^{22} cm^{-2})	$B_{\|\|}$ (μG)	$mN(\mathrm{H}_2)/B_{\|\|}$ $(2\pi G^{1/2})^{-1}$	Σ/B $(2\pi G^{1/2})^{-1}$
W3OH	50.1	3100	1.1	0.3
DR21OH1	39.8	710	3.6	0.9
SgrB2	25.1	480	3.4	0.9
M17SW	12.6	450	1.8	0.5
W3	15.8	400	2.6	0.6
S106	6.3	400	1.0	0.3
DR21OH2	20.0	360	3.6	0.9
OMC1	15.8	360	2.9	0.7
NGC2024	7.9	87	5.9	1.5
S88B	2.0	69	1.9	0.5
B1	0.8	27	1.9	0.5
W49B	0.4	21	1.2	0.3
W22	1.6	18	5.7	1.4
W40	1.0	14	4.6	1.2
ρ Oph1	0.5	10	3.3	0.8
OMCN4	12.6	$<$280	$>$ 2.9	$>$ 0.7
TauG	0.4	$<$16	$>$ 1.6	$>$ 0.4
L183	0.2	$<$16	$>$ 0.6	$>$ 0.2
L1647	1.3	$<$15	$>$ 5.5	$>$ 1.4
ρ Oph2	0.4	$<$14	$>$ 1.8	$>$ 0.5
TMC1	0.8	$<$13	$>$ 4.0	$>$ 1.0
L1495W	0.4	$<$13	$>$ 2.0	$>$ 0.5
L134	0.2	$<$11	$>$ 1.2	$>$ 0.3
TMC1C	0.8	$<$9	$>$ 5.7	$>$ 1.4
L1521	0.5	$<$9	$>$ 3.6	$>$ 0.9
L889	1.0	$<$7	$>$ 9.3	$>$ 2.3
Tau16	0.5	$<$7	$>$ 4.7	$>$ 1.2

of the column density taken along some random (slant) path will typically produce a value $mN(\mathrm{H}_2)$ that is *twice* the true surface density Σ of the flattened cloud (calculated by a perpendicular projection of the mass volume density). Making corrections of two factors of 2, we replace the fourth column by Σ/B, which is 4 times smaller than $mN(\mathrm{H}_2)/B_{||}$. [We remark that if the direction of the magnetic field is preferentially perpendicular to a sheetlike cloud, then the true value of Σ/B will instead be a factor 3 smaller than $mN(\mathrm{H}_2)/B_{||}$.] The listed values of Σ/B in the fifth column of Table 1, measured in units of $(2\pi G^{1/2})^{-1}$, are then remarkably close to the critical value of unity.

The uncertainties in the measurements and in their corrections are too great to make definitive pronouncements at the present time. The empirical evidence does appear consistent with the oft-expressed view that interstellar magnetic fields are strong enough in molecular clouds to be dynamically important. They definitely cannot be ignored. But it is premature to decide whether most clouds are magnetically supercritical or subcritical. Indeed, an interesting case can be made that molecular clouds are nearly *marginally critical.* A speculative theoretical scenario might even explain why this is the case. Perhaps all highly supercritical molecular clouds (with $\lambda \equiv 2\pi G^{1/2}\Sigma/B \gg 1$) have collapsed to form stars long ago and are no longer around to observe in the Galaxy. Perhaps highly subcritical configurations ($\lambda \ll 1$) do not become molecular clouds, because such objects must be confined against internal expansion, not by self-gravity, but largely by external pressure. Such configurations probably form diffuse clouds rather than molecular clouds. By this line of reasoning, molecular clouds capable of star formation at the present epoch of the Galaxy are self-selected to be close to being *marginally critical* . Unfortunately, for some theoretical purposes (see below), it is insufficient to deduce $\lambda \sim 1$; rather it is quite important to determine exactly on which side of $\lambda = 1$ true clouds lie.

4. Turbulent Support of Molecular Clouds

Molecular clouds are supported against self-gravity in part by turbulent motions (McKee, this volume). If turbulence and fluctuating magnetic fields make an equally important contribution to cloud support as static magnetic fields, and if the external and thermal pressures of molecular clouds can be ignored, then λ must have a value ≈ 2 (McKee 1989, Bertoldi & McKee 1992). Unfortunately, recent numerical simulations of magnetohydrodynamic (MHD) turbulence in self-gravitating molecular clouds may create problems for the point of view that turbulent pressure can be treated on an equivalent footing to microscopic thermal pressure.

A number of different groups have studied the rate of decay of strong

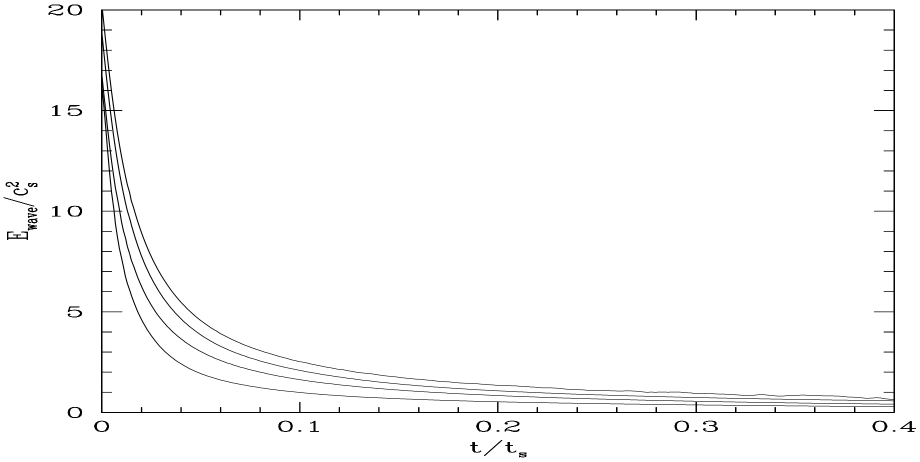

Figure 2. Free decay of total perturbed energy (turbulent kinetic energy + turbulent magnetic energy) in non-self-gravitating 3D MHD simulations. From top-to-bottom, the curves show models with $\beta \equiv c_s^2/v_A^2 = 0.01, 0.1, 1, \infty$, where c_S and v_A are respectively the sound and Alfvén speeds. The models start with saturated turbulence and wave energy per unit mass $E_{\rm wave}/c_s^2 = 20$, 19, 17, 16, with kinetic portions 13, 12, 13, 15, respectively. Time is given in units of the sound-crossing time $t_s \equiv L/c_s$ for the box. For details, see Stone, Ostriker, & Gammie (1998).

MHD turbulence, initially put into the simulations as a random collection of noncompressive motions – effectively nonlinear Alfvén waves. The original expectations were that nonlinear Alfvén waves should prove resilient to rapid dissipation since their primary fluid motion is perpendicular to the undisturbed magnetic field, and thus, they have no direct tendency to steepen and shock (Arons & Max 1975). MHD simulations with nontrivial variations only along one dimension showed that although Alfvén waves suffer a decay instability and do generate compressive motions, free MHD turbulence of a highly symmetric, primarily Alfvénic type could be relatively long-lived (Gammie & Ostriker 1996). However, calculations carried out in three dimensions (MacLow et al. 1998; Stone, Ostriker, & Gammie 1998; Padaon & Nordlund 1999) demonstrate that superpositions of nonlinear Alfvén waves with spatial variation in *all* directions couple more strongly to their fast and slow MHD counterparts. Fast and slow MHD waves generally involve compressive motions along the direction of the undisturbed magnetic field, and when they have nonlinear amplitudes, they readily shock. Figure 2 shows that the shock dissipation associated with nonlinear mode-coupling leads to a decay rate for free MHD turbulence that is almost as large for a strongly magnetized medium as for an unmagnetized one. The

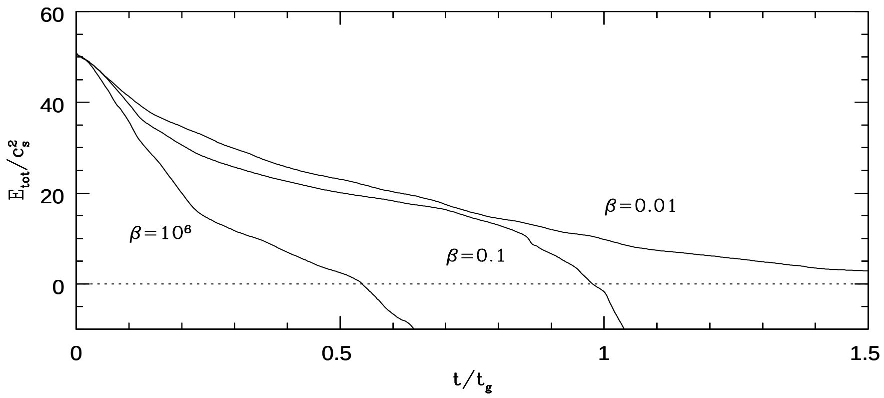

Figure 3. Free decay of total perturbed energy (turbulent kinetic energy + turbulent magnetic energy + gravitational energy) per unit mass in self-gravitating 2.5D MHD simulations with $\beta \equiv c_s^2/v_A^2 = 0.01, 0.1, 10^6$ (essentially ∞, i.e., essentially an unmagnetized cloud). All models start with perturbed kinetic energy per unit mass $(1/2)\langle v^2/c_s^2\rangle = 50$, and have box edge three times the initial Jeans length. Time is given in units of the gravitational time $t_g \equiv (\pi/G\langle\rho\rangle)^{1/2}$ where $\langle\rho\rangle$ is the mean density in the box. For details, see Ostriker, Gammie, & Stone (1999).

typical turbulent dissipation times are comparable to the fluid crossing times on the main energy-containing scale of the flow.

In following the evolution of self-gravitating clouds, an appropriate unit for measuring time is the gravitational time scale, $t_g \approx 3.3 t_{ff}$, where $t_{ff} \equiv (3\pi/32G\langle\rho\rangle)^{1/2}$ is the spherical free-fall time at the average density $\langle\rho\rangle$ of the cloud. Because turbulence lends support to clouds against collapse, their evolution must depend on the interplay of gravity and turbulent dissipation (and, potentially, turbulent re-excitation – see §6). What is the fate of a turbulent cloud, with total mass $\gg$ the thermal Jeans mass, but which is initially supported against self-gravity by a combination of turbulent motions and magnetic fields, if the turbulence undergoes free decay?

To answer this question, Ostriker, Gammie, & Stone (1999) directly simulated the evolution of self-gravitating, magnetized clouds containing an initial turbulent spectrum. Figure 3 shows the energy evolution in three such models with differing mean magnetization, and Figure 4 shows snapshots of the internal density, velocity, and magnetic field structure at successive intervals. Because observed self-gravitating clouds have flow crossing times comparable to $t_g/2$, the above-cited numerical results on turbulent dissipation suggest that the freely-decaying turbulence may not significantly

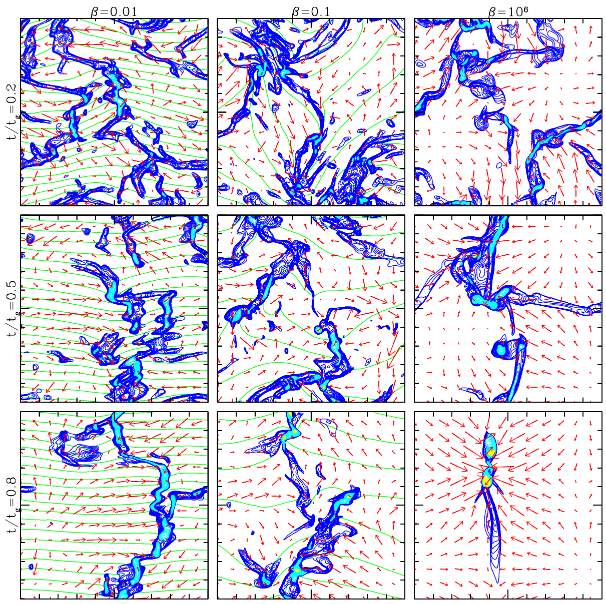

Figure 4. Snapshots of the density contours, [equally spaced by 0.1 in $\log(\rho/\langle\rho\rangle)$ starting from 0], velocity field (arrows), and magnetic field lines (light lines) at times $t/t_g = 0.2, 0.5$, and 0.8 for the self-gravitating 2.5D MHD simulations of Figure 3. For details, see Ostriker, Gammie, & Stone (1999).

prolong the support of clouds against their gravitational contraction; this is indeed the conclusion reached by direct simulations. Thus, the eventual fate of a cloud without turbulent resupply depends crucially on whether the cloud is magnetically supercritical ($\lambda > 1$) or magnetically subcritical ($\lambda < 1$). In $\lambda > 1$ clouds (e.g., the cases $\beta = 10^6$ and 0.1), Figures 3 and 4 show that the disappearance of sufficient turbulent support quickly leads to regions with overall energies that are negative and that gravitationally collapse on time scales comparable to or shorter than t_g. In $\lambda < 1$ clouds (e.g., the case $\beta = 0.01$), Figures 3 and 4 show that the removal of even all the turbulence has no such drastic effect, since the background magnetic field *by itself* suffices to prevent overall gravitational collapse. In other words, subcritical clouds can survive for times much longer than t_g, while supercritical clouds cannot, if their turbulence decays freely.

5. Filamentary Structure in Molecular Clouds

What is wrong with supposing that all molecular clouds are magnetically supercritical, and that it is the free decay of the turbulence which triggers their gravitational collapse, leading to star formation? Indeed, several recent simulations ignoring magnetic fields show highly suggestive filamentary structures to develop when clouds initially containing many thermal Jeans masses are allowed to collapse and fragment (e.g., Klessen, Burkert, & Bate 1998; Nagai, Inutsuka, & Miyama 1998). The results are similar to those obtained in cosmological studies, which provide the motivation for many of the molecular-cloud calculations.

Although filaments are observed both in the large-scale structure of the universe and in giant molecular clouds, it is unlikely that they arise from the same causes. Free gravitational collapse along the shortest available dimension (first into sheets, then into lines, then into points) is a viable option for cosmology, because the free-fall time scale $t_{\rm ff}$ in that problem is automatically of the same order as the age of the universe (in models having approximately the closure density). The average density in molecular clouds is 8 orders of magnitude times higher than the closure density of the universe; thus, the corresponding free-fall time $t_{\rm ff} \propto \langle\rho\rangle^{-1/2}$ is 4 orders of magnitude lower than the age of the universe. The conversion of large pieces of molecular clouds into stars on a time scale that approaches 3×10^6 years would yield a rate of star formation in the Galaxy that exceeds the known value (3–5 $M_\odot$ yr^{-1}) by two orders of magnitude (Zuckerman & Evans 1974). Indeed, Zuckerman & Evans's original point was that the large line-widths seen in most molecular clouds could *not* have an origin in large-scale gravitational collapse, precisely because such an interpretation would lead to far too fast a turnover of molecular gas into stars.

Figure 4 contains a possible hint why filamentation may occur in molecular clouds that do not collapse but are strongly magnetized, namely, the act of dissipating MHD turbulence creates sheetlike or filamentary clouds, with the short axis aligned preferentially along the mean magnetic field. [Turbulent MHD simulations in three dimensions show filamentary structure. The simulations of Ostriker et al. (1999) depicted in Figure 4 are two-dimensional simulations. Any feature that appears in the plane of the page is assumed to extend infinitely in the direction perpendicular to the page. Thus, what appear as filaments in the page are actually sheets.] In §7, we demonstrate via a simple toy model that turbulence driven by outflows in the directions along a sheet will naturally produce true filaments.

6. Sustenance of Cloud Turbulence Through YSO Outflows

Whether or not turbulence is essential to molecular cloud support (i.e., whether or not λ is > 1), the large line-widths observed in molecular clouds do presumably have to be sustained for periods substantially longer than $t_{\rm ff}$. It is a proposal of long theoretical and observational standing (see, e.g., Norman & Silk 1980, Lada 1985, Welch et al. 1985, Fukui et al. 1986) that the mechanism responsible for this sustenance is bipolar outflows from young stellar objects (YSOs) (Cudworth & Herbig 1979; Snell, Loren, & Plambeck 1980; Rodriguez et al. 1980). A simple calculation yields the required conditions. The equivalent of this calculation first appeared in a paper by McKee (1989; see also Gammie & Ostriker 1996).

Pudritz & Norman (1986) proposed that the back torques from a magnetocentrifugal wind can drive accretion through a disk, without the need for any anomalous viscosity (see also Wardle & Königl 1993). Many contemporary models invert this idea and suggest that YSO winds and jets are powered by magnetocentrifugally turning a fraction f of the accretion rate $\dot{M}_D$ of the disk (as set by Balbus-Hawley or self-gravitational instabilities) into a wind mass-loss rate $\dot{M}_{\rm w}$ (e.g., Shu et al. 1988, 1994a):

$$\dot{M}_{\rm w} = f\dot{M}_D. \tag{4}$$

The complementary fraction $(1-f)$ goes to building up the central star at a rate

$$\dot{M}_* = (1-f)\dot{M}_D. \tag{5}$$

If f is the same for all YSOs, we may temporarily take $\dot{M}_*$ to represent, not the mass-accumulation rate of any given YSO, but the rate at which molecular cloud gas is being converted by gravitational collapse into stars *throughout the whole Galaxy.* The symbol $\dot{M}_{\rm w}$ would then represent the global rate at which YSO winds and jets are injecting material back to the interstellar medium (mostly molecular clouds since the heaviest mass-loss rates apply to the deeply embedded phases). The relation between $\dot{M}_{\rm w}$ and $\dot{M}_*$ for a single star or for the whole Galaxy then reads

$$\dot{M}_{\rm w} = \left(\frac{f}{1-f}\right)\dot{M}_*. \tag{6}$$

We assume that these YSO winds and jets have typical terminal velocities $v_{\rm w}$. The total momentum input per unit time into all the molecular clouds of the Galaxy from YSO winds and jets is then

$$\dot{M}_{\rm w} v_{\rm w} = \left(\frac{f}{1-f}\right)\dot{M}_* v_{\rm w}. \tag{7}$$

The corresponding energy injection rate into the cloud is

$$\frac{1}{2}\dot{M}_{\rm w} v_{\rm w} v_{\rm sh} = \frac{1}{2}\left(\frac{f}{1-f}\right)\dot{M}_* v_{\rm w} v_{\rm sh}, \tag{8}$$

where $v_{\rm sh}$ is the mean outflow shell speed. This rate must be smaller than the energy flux in the YSO outflows themselves, because the outflow-cloud interaction is probably momentum- rather than energy-conserving (see Lada 1985).

In contrast, the dissipation rate of the energy contained in cloud turbulence which is forced on a scale ℓ equals

$$\frac{M_{\rm GMC} v_{\rm turb}^2}{2t_{\rm diss}}, \tag{9}$$

where $M_{\rm GMC}$ is the total mass of giant molecular clouds (GMCs) in the Galaxy, $v_{\rm turb}$ is the typical turbulent velocity inside a GMC, and $t_{\rm diss} \approx \ell / v_{\rm turb}$ is the usual hydrodynamic time scale for turbulent dissipation and does not differ much for MHD turbulence according to the numerical simulations described in Figure 2. In steady state, we assume the energy input rate (8) is balanced by the dissipation rate (9); this yields the level of turbulence that can be maintained by YSO winds and jets:

$$v_{\rm turb} = \left(\frac{f}{1-f}\right)^{1/3} \left(\frac{\dot{M}_* \ell v_{\rm sh}}{M_{\rm GMC} v_{\rm w}^2}\right)^{1/3} v_{\rm w}. \tag{10}$$

With the substitutions, $M_{\rm GMC} \approx 10^9\ M_\odot$, $\dot{M}_* \approx 4\ M_\odot\ {\rm yr}^{-1}$, $v_{\rm w} \approx 200$ km s^{-1}, $\ell \approx 1$ pc, and $v_{\rm sh} \approx 10$ km s^{-1}, we obtain the numerical value,

$$v_{\rm turb} \approx \left(\frac{f}{1-f}\right)^{1/3} 2\ {\rm km\ s}^{-1}. \tag{11}$$

Notice that the expression (10) is relatively insensitive to the product of the length and velocity scales, $\ell v_{\rm sh}$, where the energy input from YSO outflows is assumed to couple into the turbulent velocity field.

The X-wind model predicts that $f \approx 1/3$ (see §12 below), which yields a value from equation (11) for $v_{\rm turb}$ sustainable by YSO outflows that is compatible with the 1–2 km s^{-1} actually seen in the line-widths of typical GMCs. A wind efficiency this large (where for every solar mass of material that goes into a star, roughly half a solar mass is shot back out at 200 km s^{-1}) has been claimed only for the X-wind model (cf. Shu et al. 1988, 1994a). Indeed, there is probably no source of mechanical energy in the Galaxy except for material flung from the near-vicinity of stellar surfaces that could come remotely close to replenishing the energy drain represented by the dissipation of molecular cloud turbulence.

7. A Toy Model of GMC Structure and Evolution

In the directions across magnetic fields, giant molecular clouds measure tens of parsecs, and clumps within them measure from a fraction to a few parsecs (Blitz, this volume). How thick are molecular clouds along the direction of the mean field? At first sight, the situation appears simple from a theoretical perspective. If thermal pressure is the only means of support against self-gravity in the direction of the mean field, then the density half-height of a layer with isothermal sound speed a and surface density Σ is given by Spitzer's (1942) formula:

$$z_0 = \frac{a^2}{\pi G \Sigma} \tag{12}$$

For $T = 10$ K and $m = 2.4\ m_{\rm H}$ (corresponding to $a = 0.2$ km s^{-1}), and $\Sigma = 0.01$ g cm^{-2} (corresponding to 2.5 mag of visual extinction), equation (12) yields $z_0 = 0.06$ pc. Under such circumstances, GMCs and cloud clumps should essentially be sheets (Pudritz 1986).

Internal turbulence thickens the cloud in the direction parallel to the mean magnetic field (Arons & Max 1975), whereas the extra magnetic pressure above and below the cloud resulting from field lines bending to support the cloud in the lateral direction (e.g., Li & Shu 1996) and converging turbulent flows exterior to a cloud clump (e.g., Fig. 4) would make the sheet locally even thinner than indicated by equation (12). Shu, Adams, & Lizano (1987) noted that bipolar outflows are often aligned with the ambient magnetic field (Vrba, Strom, & Strom 1976; Akeson & Carlstrom 1997), and some of these flows are still within the cloud after sweeping ambient molecular gas out to a parsec. On the other hand, Reipurth, Bally, & Devine (1997) discuss examples of parsec-long optical jets from YSOs that have clearly broken out of their local natal clouds. Thus, the question of how spatially thick are clouds in the direction parallel to the mean magnetic field remains open both theoretically and observationally.

In the rest of this section, we adopt as a toy model the hypothesis that molecular clouds are spatially flat sheets. We allow for self-gravity, magnetic fields (static or not), and fluid motions (turbulent or not as long as they take place only in the plane of the sheet), but we suppose that thermal pressure is negligible at the relatively large scales ($\gg 0.1$ pc) of primary interest here. We further suppose that the local mass-to-flux ratio has a spatially constant value:

$$\frac{\Sigma}{B_z} \equiv \Lambda = \text{const}, \tag{13}$$

where z is the direction normal to the sheet and B_z equals the total B at the midplane. If field freezing holds, then the ratio Σ/B_z is also temporally constant at the value Λ as the sheet evolves in the x–y plane.

As before, it is convenient to introduce the symbol λ for the dimensionless mass-to-flux ratio:

$$\lambda = 2\pi G^{1/2}\Lambda. \tag{14}$$

Shu & Li (1997) call a magnetized sheet with a spatially and temporally constant value of λ *isopedic*. For an isopedic sheet, they showed that for arbitrary variations of $\Sigma(x, y, t)$, the magnetic forces exerted in the plane of the sheet are a (negatively) scaled version of self-gravity, with the constant of proportionality equal to $-1/\lambda^2$. An especially interesting situation occurs if the sheet is critically magnetized. *If $\lambda = 1$, then magnetic forces exactly balance gravitational forces everywhere in the sheet, independent of how complex are the motions and density (and field) distributions.* Since we have ignored the effects of thermal pressure (which requires for self-consistency that we also ignore the magnetic pressure but not the magnetic tension), this means that the equations of motion are especially simple: Small pieces of the sheet move at constant speed in a straight line until they collide with other small pieces of the sheet. (Recall that there are no other forces in the problem if we explicitly treat the turbulent motions as actual motions rather than as some sort of artificial eddy stress.) When different pieces of the sheet do collide, the shock jump conditions (for a zero temperature sheet) are also simple: The collision occurs inelastically, with the conservation of total mass and vector momentum of the various pieces and with the removal of all relative motion along the line of centers after the pieces coagulate.

Clearly, if there is continual dissipation of energy when pieces of the sheet intersect, any initial velocity field containing differential motions would tend to resolve itself into narrow dense regions ("filaments") where opposing pieces of the sheet have collided inelastically, merged, and are now traveling together in a common direction. The self-gravity in the dense filaments would be intense, but it would be balanced by an opposite and equally intense magnetic tension created by all the field lines that thread through the individual pieces and have now been bunched together tightly in the midplane while they spread out quickly above and below the sheet. The prediction that magnetic field lines thread mainly *perpendicularly* (in a cylindrical fan above and below the sheet) to the long axes of well-defined filaments distinguishes our theory from several of its competitors.

The exact balance would be lost, however, if the condition of field freezing breaks down. Realistically, we expect ambipolar diffusion and thermal pressure (relative to "turbulent pressure") to become important effects when cloud surface and volume densities rise beyond certain values (see Lizano & Shu 1989 and §8). For purposes of the simulations that follow, let us somewhat arbitrarily suppose that ambipolar diffusion becomes very efficient when the local surface density, averaged over a unit cell (representing a molecular cloud core of typical diameter 0.1 pc) in a grid-based scheme, rises to 100 times the global average value. We then suppose that the affected gas loses its magnetic support and forms stars.

In the displayed simulations, when a cell acquires 400 particles in any given time step, 32 particles are assumed to form one or more stars; 16 particles [corresponding to $f/(1-f) = 16/32 = 1/2$, i.e., to a wind fraction $f = 1/3$] are ejected in the form of a bipolar wind with a terminal velocity $v_{\rm w}$ equal to 230 km s^{-1}. The corresponding momentum input, 3680 particle km s^{-1}, is immediately shared by the 368 ambient particles in the cell (16 in the original wind plus 352 in the cell that did not participate in the gravitational collapse but got swept up in the outflow); thus, a molecular outflow of 10 km s^{-1} carried by these 368 particles impinges on neighboring cells as a result of the star-formation process in any dense core. Although the mass scale can be chosen arbitrarily, for definiteness we may imagine the original 400 particles to represent the typical 11 $M_\odot$ core that Onishi et al. (1998) find per star-forming event in the Taurus molecular cloud.

To keep the problem (artificially) two-dimensional, we suppose that the outflow is ejected within wedges of opening angle 45° aligned in two diametrically opposed directions in the plane of the sheet. On the rationale that stars are unlikely to form exactly in the midplane of the sheet, the orientation of the bipolar outflow axes is taken to be parallel to the local direction of the horizontal component of the magnetic field just above and below the midplane of the sheet. The underlying assumption is that the outflow axis lies along the spin angular momentum vector of (the inner edge of) the accretion disk (see §12), whereas magnetic braking of the pre-collapse cloud tends to align the spin vector parallel to the local direction of the interstellar magnetic field **B** (see Mouschovias & Paleologou 1980 for relative efficiencies of braking for the parallel and perpendicular rotators). Thus, YSO outflows should have a tendency to align with **B** in the ambient medium. This orientation rule yields the only reason for calculating the geometries of the gravitational and magnetic fields, since, in their dynamical influence on the remaining gas, they are always assumed to balance.

The last assumption breaks down if a significant fraction of the total mass becomes locked up in stars, with the corresponding magnetic flux released (rather than destroyed) back into the remaining gas. Fortunately for the meaningfulness of the simulations, the star formation rate is low (with the assumption that ambipolar diffusion becomes fast only when the local surface density rises to 100 times the global average), and the fundamental assumption of strict force-balance becomes bad only after about 50 Myr, when about 40% of the mass of the original cloud has turned into stars (giving a time scale 50 Myr/0.4 = 125 Myr for gas consumption equal to half the global average of $M_{\rm GMC}/\dot{M}_* = 10^9\ M_\odot/4\ M_\odot$ yr^{-1}).

We follow the fate of the ejected wind by the same dynamic rules as the cloud gas. Thus, the bipolar outflows sweep up ambient gas into thin moving shells that obey vector momentum conservation. This process resupplies the "turbulence" that is lost elsewhere through inelastic collisional

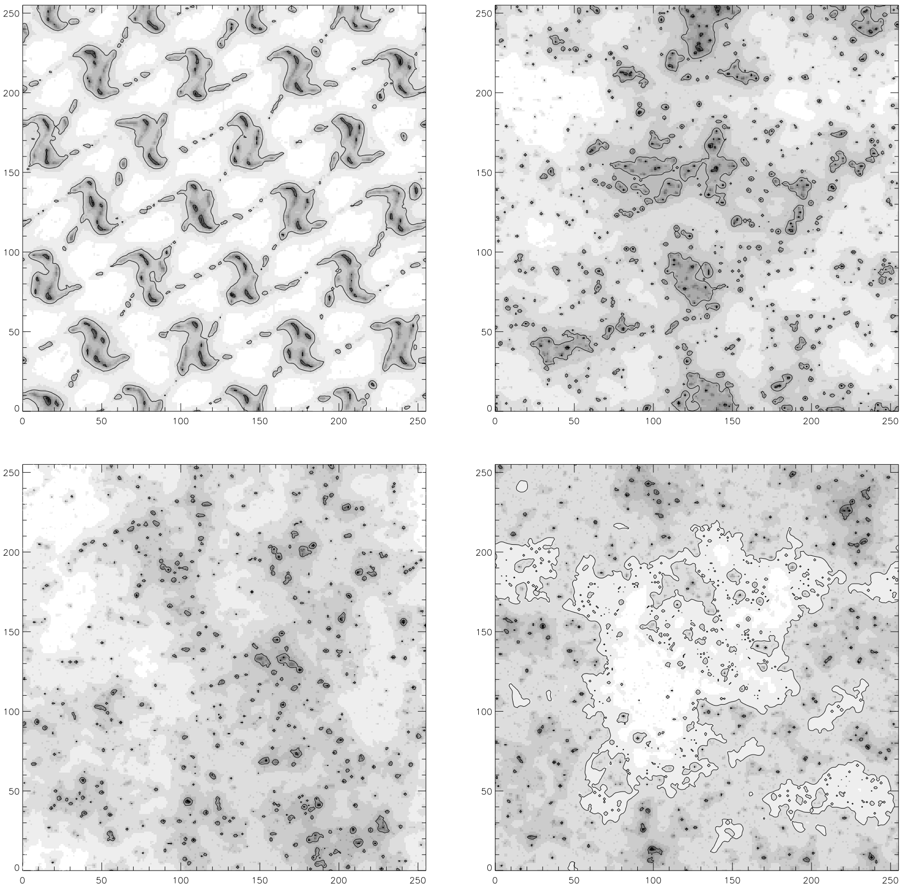

Figure 5. Equipotential plots of toy model simulation of the evolution of a $\lambda = 1$ molecular cloud sheet. The upper left panel corresponds to a time of 2.5 Myr; the upper right panel, to a time of 15 Myr; the lower left panel, to 28 Myr; and the lower right panel, to 50 Myr. For details, consult Allen & Shu (1999a).

agglomeration. The individual moving shells also eventually merge to form new dense filaments and cores that give rise to further generations of young stars and outflows.

Figure 5 shows the evolution of a toy-model simulation with periodic boundary conditions (Allen & Shu 1999a). The computations are done on a 256×256 grid, with each cell measuring 0.1 pc along the x and y lengths. Contours of gravitational equipotential are plotted on a grey scale; iso-surface-density contours would look similar, but less smooth with the number of gas particles ($4 \times 256 \times 256$) used in the simulation. The simulations are started with a uniform and smooth surface density distribution, except that the 4 particles in each cell are given random spatial positions. They are also given small x and y velocities (of order 1–2 km s^{-1}) that vary sinusoidally with spatial position.

The upper left panel of Figure 5 yields the configuration after 2.5 million years (2.5 Myr) of evolution. The pattern looks like wallpaper, with strict periodicity destroyed only by the small random elements introduced in the initial conditions. The system quickly loses all memory of such artificialities.

After 15 Myr of evolution, the configuration looks as displayed in the upper right panel. Small dense cores have formed that have given birth to stars with outflows. The outflows replenish the "turbulent" motions, but in an anisotropic fashion, since they are directed along the x–y direction of the mean magnetic field above and below the midplane. These directions can be read off the figures by noting that the magnetic field $\mathbf{B}$ is locally parallel (or antiparallel) to the gravitational field $\mathbf{g}$ everywhere, and the components of $\mathbf{g}$ (in the x and y directions) are, of course, perpendicular to the equipotential contours that are being plotted in Figure 5.

The eye easily picks out "filaments" in all of the three later figures. The filaments are dotted by dense cores along their length. We believe that filaments form by the following "instability" process, but we do not have yet a quantitative analysis. Once there is any tendency for elongation in the x–y plane, the associated magnetic field orientations favor outflows that are directed along the short axis of that elongation. (For a vivid demonstration that nature might have reproduced this tendency, see Yu, Bally, & Devine 1997.) These bipolar outflows then sweep up ambient gas that also tends to form elongated structures with similar spatial orientations. Two adjacent parallel filaments firing outflows at each other reinforce the compressional tendency, although they also ultimately blast each other apart.

The lower left panel of Figure 5 shows the situation after 28 Myr. Long irregular filaments studded with dense cores are apparent. The overall impression is not qualitatively dissimilar to observational maps of the Taurus molecular cloud complex (cf. Myers 1995, Mizuno et al. 1995). Although cloud filaments and cloud fragments exist throughout the map, notice that the overall region is in (neutral) force balance. Gravitational collapse is not occurring anywhere except at the centers of the densest cloud cores.

The lower right panel depicts the configuration after 50 Myr, when 40% of the original mass of the cloud has been turned into stars, which are distributed more or less uniformly throughout this region (although some have migrated out of the original computational area, to be replaced by stars from neighboring areas because of the periodic boundary conditions). The gas has been pushed by outflows in the interior toward the edges of the computational box, but the periodic boundary conditions, of course, prevent any permanent loss of gas from the region.

The toy model introduced above clearly has its limitations when we attempt to apply it to the real world. Removing some of these limitations (e.g., the periodic boundary conditions) would not represent hard work; removing others (e.g., the two-dimensionality of the calculations) would require abandoning simplifying basic properties of the toy model [e.g., the Shu & Li (1997) theorems] and would add considerable computational effort. Despite its weaknesses, however, our toy model may contain some elements of essential truth. In particular, we believe that it yields a highly suggestive mechanism for the formation of filamentary clouds that does not require global free-fall gravitational collapse and fragmentation with its attendant untenably high rates of star formation.

8. Formation and Evolution of Molecular Cloud Cores

Low-mass stars form in the dense cores of molecular clouds (Myers & Benson 1983, Mizuno et al. 1994, Myers 1995). These cores have a typical size ~ 0.1 pc, a number density $\sim 3 \times 10^4$ cm^{-3} or greater, a mass ranging from a fraction of a solar mass to about 10 $M_\odot$, and an axial ratio for flattening of typically 2:1. For isolated cores, the last fact implies that agents other than isotropic thermal or turbulent pressures help to support cores against their self-gravity, although it is not yet clear observationally whether the true shapes are oblate, prolate, or triaxial (Myers 1998, personal communication). Observed cloud rotation rates are generally too small to account for the observed flattening (Goodman et al. 1993). This leaves magnetic fields, which are believed for other reasons to play a crucial role in contemporary star formation.

In one scenario, the weakening of magnetic support by ambipolar diffusion (Mestel & Spitzer 1956) leads to the continued contraction of a cloud core with ever growing central concentration (Nakano 1979, Lizano & Shu 1989, Basu & Mouschovias 1994). On a time scale given by the core scale length divided by the characteristic slip velocity between ions and neutrals, the molecular cloud core reaches a "gravomagneto catastrophe" where the central density formally tries to reach infinite values. Shu (1995) pointed out that the process has some features in common with the "gravothermal catastrophe" (Lynden-Bell & Wood 1968, Lynden-Bell & Eggleton 1980, Cohn 1980) that overtakes globular-cluster core-evolution because of the diffusion of random velocities by stellar encounters.

Myers (this volume) points out that inward fluid velocities of magnitude ~ 0.1 km s^{-1} exist at large radii in some starless cores, and that this feature is not predicted by any of the ambipolar-diffusion calculations cited above (see also Onishi, Mizuno, & Fukui 1999). Myers suggests instead that pre-existing inward motions prior to true gravitational collapse and star for-

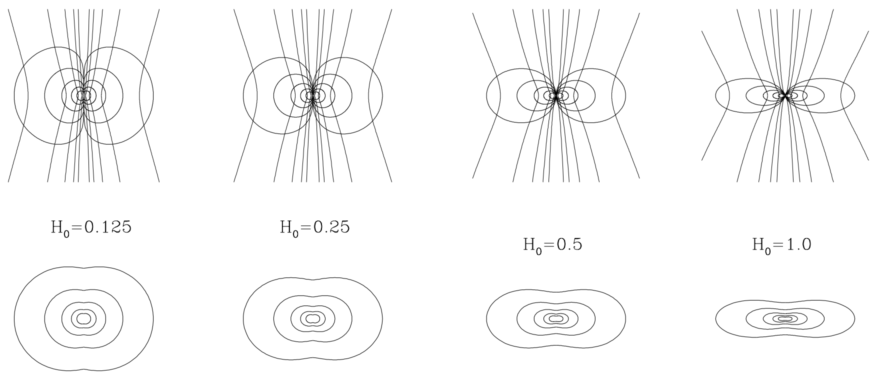

Figure 6. Isodensity contours and magnetic field lines of isopedic singular isothermal toroids for values of the over-density parameter $H_0 = 0.125,\ 0.25,\ 0.5,\ 1.0$. The corresponding values of λ are $\lambda = 8.38, 4.51, 2.66, 1.79$. Below each plot is the equator-on projection of the column density. For details, consult Li & Shu (1996).

mation are better modeled as resulting from the decay of turbulence (see also Nakano 1998). Figure 2 of Lizano & Shu (1989) lends quantitative credence to this suggestion (see also Myers & Lazarian 1998). If the sequence of decaying turbulent parameter $K = 12, 10, 6, 2$ in the cited Figure were to occur over $\sim$ a few Myr, then inward motions of order $0.5a \sim 0.1$ km s^{-1} could indeed be generated at distances of order 0.1 pc from the center of the cloud core. Such subsonic motion and the generally shorter time scale may distinguish the "gravoturbo catastrophe" resulting from the decay of turbulence in a pre-existing, magnetically supercritical, core with $\lambda > 1$ from a core that reaches supercriticality via the "gravomagneto catastrophe" produced by ambipolar diffusion.

9. The Pivotal State

Li & Shu (1996) termed the cloud configuration when the central isothermal concentration first becomes formally infinite as the "pivotal" state ($t \equiv 0$). This state separates the nearly quasistatic phase of core evolution ($t < 0$) that leads to gravomagneto or gravoturbo catastrophe ($t = 0$) from the fully dynamic phase of protostellar accretion ($t > 0$). (See the first two stages depicted in Fig. 7 of Shu, Adams, & Lizano 1987.) The numerical simulations indicate that the pivotal states have a number of simplifying properties, which motivated Li & Shu to approximate them as scale-free equilibria with the power-law radial dependences for the density and magnetic flux function:

$$\rho(r,\theta) = \frac{a^2}{2\pi G r^2} R(\theta), \qquad \Phi(r,\theta) = \frac{4\pi a^2 r}{G^{1/2}} \phi(\theta). \tag{15}$$

In equation (15), we have adopted a spherical polar coordinate system (r, θ, φ), and a is the isothermal sound speed of the cloud, while $R(\theta)$ and $\phi(\theta)$ are the dimensionless angular distribution functions for the density and magnetic flux given by force balance along and across field lines. The resulting differential equations and boundary conditions yield a linear sequence of possible solutions, characterized by a single dimensionless free parameter, H_0, which represents the fractional overdensity supported by the magnetic field above that supported by thermal pressure. Comparison with the typical degree of elongation of observed cores suggests that the overdensity factor $H_0 \approx 0.5 - 1$ (corresponding to $\lambda \approx 2$).

In Figure 6, we plot isodensity contours and field lines for the cases $H_0 =$ 0.125, 0.25., 0.5, 1.0. Below each case are the column density contours that would be seen by an observer in the equatorial plane of the configuration. The presence of very low-density regions at the poles of the density toroid has profound implications for the shape and kinematics of bipolar molecular outflows. [See also Torrelles et al. (1983, 1994).]

10. Self-Similar Collapse of Singular Isothermal Toroids

It is well-known that the collapse of the singular isothermal sphere (corresponding to the case $H_0 = 0$ in the previous section) occurs in a *self-similar* manner (Shu 1977). The same holds true for any member in the sequence of isopedically magnetized singular isothermal toroids. For given H_0, we have only two dimensional parameters in the problem, a and G. From a and G, we cannot form dimensions for all required physical quantities without using the independent variables of the problem themselves: r, θ, and t. The quantities r and at both have the dimensions of length, and they can be combined to form the dimensionless similarity variable

$$x = r/at, \tag{16}$$

which can then appear, along with θ, as the argument for nondimensional mathematical functions. Thus, the time-dependent solution that describes the $t > 0$ evolution of the unstable equilibrium state (15) must take the *self-similar* form:

$$\rho(r,\theta,t) = \frac{\alpha(x,\theta)}{4\pi G t^2}, \quad \mathbf{u}(r,\theta,t) = a\mathbf{v}(x,\theta), \quad \mathbf{B}(r,\theta,t) = \frac{a}{G^{1/2} t}\mathbf{b}(x,\theta), \tag{17}$$

where $\mathbf{u}$ and $\mathbf{B}$ are the poloidal fluid velocity and magnetic field, respectively. The dimensionless dependent variables $\alpha(x,\theta)$, $\mathbf{v}(x,\theta)$, and $\mathbf{b}(x,\theta)$

are called the *reduced* density, velocity, and magnetic field. Solutions with the form (17) are called "self-similar" because, apart from a simple scaling of dependent and independent variables, the solution at one instant in time looks the same as the solution at another instant in time.

For the case $H_0 = 0$ (corresponding to $\mathbf{b} = 0$), we may assume that the flow occurs spherically symmetrically. With no θ dependence and with $\mathbf{v}$ having only a radial component, the similarity solution has an easy description. At $t = 0^+$, consider initiating collapse of the densest innermost portions of a (nonrotating and unmagnetized) singular isothermal sphere to form a condensed central object (a protostar, whose physical dimensions are so small as to allow us here to approximate it as a point mass). An observer located in the outer portions of the cloud does not realize anything has happened gravitationally, because Newton's theorem for the gravitational field of spherical objects misleads the observer into thinking that all the mass interior to the observer's location equivalently lies at the center anyway. Only when a sound wave traveling outwards at the speed a reaches the observer, does the observer realize, hydrodynamically, that the bottom has dropped out. The information propagates outward, initiating a wave of falling whose location at time t has a head described by the locus $r = at$. The similarity variable description for the same locus is $x = 1$. For x larger than 1 (or $r > at$), the density profile retains its unperturbed value $\alpha = 2/x^2$ (or $\rho = a^2/2\pi G r^2$), and the fluid is at rest, $\mathbf{v} = 0$ (or $\mathbf{u} = 0$).

The solution interior to the head of the expansion wave is modified from the initial state (see Shu 1977). At $x = 1$, the solutions for α and v connect without a jump, but with a discontinuous first derivative (because of the presence of the head of the wave) to the unperturbed state corresponding to the singular isothermal sphere. Near the origin, the solutions take the asymptotic forms,

$$\alpha \to \left[\frac{m_0}{2x^3}\right]^{1/2}, \qquad v(x) \to -\left[\frac{2m_0}{x}\right]^{1/2}, \qquad \text{as} \qquad x \to 0, \tag{18}$$

that correspond to gravitational free-fall onto a (reduced) central mass found by numerical integration to be $m_0 = 0.975$. In dimensional units, the origin contains a central mass point (star) that grows linearly with time:

$$M_* = m_0 \frac{a^3 t}{G}. \tag{19}$$

Equation (19) constitutes the most important property of the solution – the conclusion that the gravitational collapse of a singular isothermal sphere yields, not a characteristic mass, but a characteristic *mass infall rate* given by

$$\dot{M}_{\rm in} = m_0 \, \frac{a^3}{G}. \tag{20}$$

For $a = 0.2$ km s^{-1} (Taurus region), $\dot{M}_{\rm in} \approx 2 \times 10^{-6}\ M_\odot$ yr^{-1}. The time t required to build the typical T Tauri star of mass $0.5\ M_\odot$ is then 2.5×10^5 yr. The ratio of this time scale (for gravitational collapse before the complete reversal of the infall) to the mean age of T Tauri stars agrees reasonably well with the ratio of the numbers of embedded (Class I) sources to the numbers of the revealed (Class II) sources in the Taurus cloud. A review of more direct observational tests of theoretical collapse models is given by Evans (1999).

Inclusion of the effects of finite levels of the magnetic field (i.e., $H_0 \neq 0$) does not change the qualitative situation. The collapse still occurs self-similarly from "inside-out," but the departures from spherical symmetry implies that non-zero motions can be induced *gravitationally* ahead of the front of the expansion wave (see also Terebey, Shu, & Cassen 1984 for the case when the cause of departure from spherical symmetry is rotation). If the gravitational precursor motions are sufficiently compressive, the expansion wave, now propagating outward at the fast MHD speed, may even be preceded by a weak shock wave (Li & Shu 1997). But the main new feature introduced by the presence of the magnetic field is a flattening of the flow in the inner regions to form a "pseudodisk" (see the perturbational treatment by Galli & Shu 1993a,b of this problem).

Figure 7 is obtained by applying the ZEUS 2-D MHD code (Stone & Norman 1992) to the collapse of a singular isothermal toroid with $H_0 = 0.25$ (Allen & Shu 1999b). The computations are carried out in the usual time-dependent way, without making use of the similarity assumption. The results at time intervals of $\Delta t = 2 \times 10^{12}$ s are displayed as contour plots in the meridional plane of the similarity coordinates ϖ/at and z/at. If the numerical calculations were infinitely precise, the contours for α, $|\mathbf{v}|$, and $|\mathbf{b}|$ at different times t would all lie on top of one another, defining the exact similarity solution. Because of errors associated with finite differencing, the contours at different t do *not* lie exactly atop one another, with the errors being larger at earlier times than later ones since the nontrivial part of the flow is spanned by more grid points at later times. Thus, unlike most numerical simulations which degrade with the passage of time, these simulations get better with time, and the computed values at $t = 8 \times 10^{12}$ s (the only case for which unit vectors showing the directions of $\mathbf{v}$ and $\mathbf{b}$ are displayed) have essentially converged on the correct self-similar values.

Since unstable cloud cores probably have dimensionless mass-to-flux ratios $\lambda = 1$–3, whereas T Tauri stars have $\lambda > 5000$, the assumption of field freezing must break down at high collapse densities (Nakano & Umebayashi 1980, Li & Shu 1997). Whether flux loss in forming protostars ultimately occurs by magnetic reconnection (e.g., Mestel & Strittmatter 1967, Galli & Shu 1993b) or by C-shocks (Li & McKee 1996, Li 1998a, Ciolek & Königl

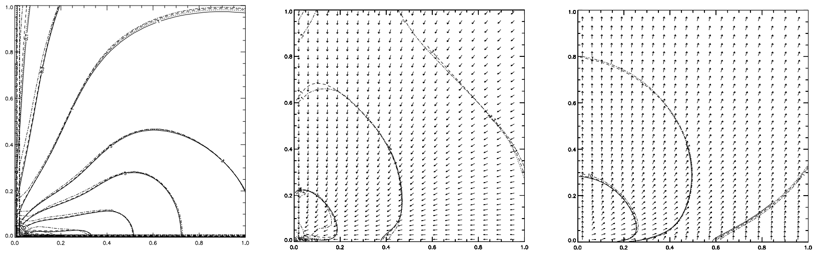

Figure 7. The reduced density α (left panel), velocity $\mathbf{v}$ (middle panel), and magnetic field $\mathbf{b}$ (right panel) plotted at time $t = 2, 4, 6, 8 \times 10^{12}$ s in the meridional plane of the similarity coordinates (ϖ/at)–(z/at). The curves give contours lines of equal density, speed, and field magnitude in intervals of 0.5 dex, while the arrows give unit vectors of the directions (on grid points) for the fluid velocity and magnetic field. For details, consult Allen & Shu (1999b).

1998) remains to be seen. Self-similar collapse calculations carried out with the assumption of strict field freezing yield important "outer solutions" for computations of the flux-loss problem in the inner regions (e.g., Li 1998b).

There is another important lesson to be learned from the self-similar collapse calculations. Contrary to earlier speculations made in the literature, magnetic tension in the envelope never suffices to hold up the envelope against the gravity of the growing protostar. When the wave of infall reaches successively larger portions of the envelope, those portions move inward to fill the hole and become part of the infalling material. In the specific case of the magnetized singular isothermal toroid, without some other influence, the mass infall rate into the central regions continues indefinitely at the constant rate given by equation (20), with the coefficient m_0 given numerically by $m_0 = 0.975(1 + H_0)^2$ when $H_0 \ll 1$ (Allen & Shu 1999b) and by $m_0 = 1.05(1 + H_0)$ when $H_0 \gg 1$ (Li & Shu 1997). In all cases, the inclusion of the effects of magnetic forces (when $H_0 > 0$) *increases* the rate of central mass accumulation in comparison with the nonmagnetized case ($m_0 = 0.975$), and does not decrease it. The main reason for the increase is that the cloud core is denser on average before it begins to collapse when supported by magnetic fields than when this support is absent. The slowing down of the infall speed by magnetic forces once collapse begins is largely offset by the increase of the signal speed at which the wave of infall propagates outward (Galli & Shu 1993a,b).

Influences other than magnetic fields can also quantitatively affect the mass infall rate, $\dot{M}_{\rm in}$, i.e., the rate at which the central YSO accumulates matter. For example, turbulence modeled by an isotropic pressure $P_{\rm turb}$ can also help to support a cloud core against its self-gravity. Approximated as a polytrope ($P_{\rm turb} \propto \rho^{\Gamma}$) or as a logatrope ($P_{\rm turb} \propto \ln \rho$), self-gravitating, turbulent, cloud cores can acquire pivotal states with density laws that depart from the $\rho \propto r^{-2}$ dependences that have become familiar for isothermal configurations (e.g., Lizano & Shu 1989, McLaughlin & Pudritz 1997, Galli et al. 1999). The gravitational collapse of such configurations will also yield mass infall rates $\dot{M}_{\rm in}$ that are not constant in time, just as pre-existing inward motions at the pivotal instant $t = 0$ in magnetized isothermal configurations will yield non-constant mass-infall rates (Basu 1997, Ciolek & Königl 1998, Li 1998a). When added to the support provided quasistatically by thermal pressure, all of these mechanisms *increase* the mass infall rate above the base value given by the inside-out collapse solution for the singular isothermal sphere: $\dot{M}_{\rm in} = 0.975a^3/G$. None of the considerations imply that $\dot{M}_{\rm in}$ should *cut off* after some definite time and leave us with a star with a well-defined mass.

To obtain a stellar mass scale, one of three things might happen. First, the growing star might run out of matter to accumulate. The wave of infall might run into a vacuum because the material previously there has already fallen into some other star. This alternative requires the star formation process to be nearly 100% efficient, which we know is not the case except, possibly, in the relatively rare (at present) cases of bound cluster formation.

Second, the star might move out of its surrounding cloud core. In isolated regions of star formation, it is difficult to imagine how this occurs since the pit in the potential (where presumably the star forms) must move nearly with the center of mass of the core. In more crowded environments, a formed star might be freed from the gas dynamical forces that constrain the motion of its surrounding cloud core, and thus under the gravitational influences of the rest of the system, the star might begin to move differently from its parent core. However, the virial velocity gained by the star this way will be only comparable to, and not much larger than, the virial velocity $a_{\rm eff}$ (with contributions from thermal pressure, magnetic effects, and turbulence) that supports the gas against the self-gravity of the system. The resulting mass-infall rates by Bondi-Hoyle accretion will then not differ much from the canonical formula $a_{\rm eff}^3/G$, unless the star-formation process has been pretty efficient, and there is not much cloud gas left in the spaces between already formed stars.

Third, the material otherwise destined to fall onto the star might be removed by some hydrodynamic, magnetohydrodynamic, or photevaporative process. Obvious candidates are mechanisms that involve energetic massive stars: HII regions, supernova explosions, etc. Observations of YSOs, however, offer an even more intriguing possibility: outflows from the central

YSO itself. Indeed, it is an empirical fact that no embedded protostar has yet been found to reveal itself as an optical object without first developing an outflow. This fact strongly suggests that stars help to define their own mass by YSO winds that reverse the continuing infall which would otherwise continue to build up the mass of the central object to ever higher masses (Shu & Terebey 1984).

The above conjecture does not mean that the interstellar medium plays *no* role in helping to define stellar masses. On empirical grounds it has been argued for some time (see, e.g., Shu, Adams, & Lizano 1987; Myers, Ladd, & Fuller 1991; Myers 1995; Shu 1995) that high-mass stars form from cores that produce high rates of infall $\dot{M}_{\rm in}$, whereas low-mass stars form from cloud cores that produce low rates of infall, consistent with the observation that the regions which form high-mass stars are more turbulent and hotter than the regions that form low-mass stars. In particular, Myers & Fuller (1993) have proposed that stars from 0.3 to 30 $M_\odot$, take about the same time to form, about 10^5 yr. This simple prescription corresponds to $\dot{M}_{\rm in} \propto M_*$, where M_* is the final stellar mass. Presumably, since the determination of M_* (end of collapse) comes after the determination of $\dot{M}_{\rm in}$ (beginning of collapse), a high value of $\dot{M}_{\rm in}$ *causes* a high value for M_*.

To close the logical loop, if we believe that it is outflows that sets final stellar masses, then it must also be true that stars of all masses have sufficient wind power $\dot{M}_{\rm w}$ to reverse the infall $\dot{M}_{\rm in}$ that makes them. This will require higher-mass stars to have more powerful outflows than lower-mass stars. Qualitatively, observations appear consistent with this requirement (see, e.g., Bally & Lada 1993). But quantitatively, can we make a theoretical case that $\dot{M}_{\rm w}$ increases (more or less linearly) as $\dot{M}_{\rm in}$ increases? As we shall see in the section after next, an attractive feature of X-wind theory is that it has precisely this property.

11. Mass Loss from Stars and Disks

Strong magnetic fields can considerably enhance the mass loss $\dot{M}_{\rm w}$ of thermally driven winds from the surfaces of rapidly rotating stars (Mestel, 1968). Even if the resultant flow is quite cold, Hartmann & MacGregor (1982) demonstrated that $\dot{M}_{\rm w}$ could have almost arbitrarily large values, dependent only on the ratio of the azimuthal and radial field strengths at the position where the gas is injected onto open field lines near the equator of a protostar that rotates near breakup. Shu et al. (1988) assigned the cause for the protostar to spin at breakup to a circumstellar disk that abuts against the surface of the central object and accretes onto it at a high rate $\dot{M}_D$. They also replaced Hartmann & MacGregor's arbitrary angle of injection for gas velocity and magnetic field direction with the requirement that in steady state, the wind mass-loss rate must be a definite fraction f of the disk accretion rate $\dot{M}_{\rm w} = f\dot{M}_D$ (see below). [In steady state, $\dot{M}_D$ should equal $\dot{M}_{\rm in}$. However, with the passage of time, the outflow may reduce the effective infall rate $\dot{M}_{\rm in}$ below the undisturbed rate (20) had the outflow not been present.]

Blandford & Payne (1982) advanced an influential self-similar model of centrifugally driven winds from the surfaces of magnetized accretion disks. Pudritz & Norman (1983) applied these pure disk-wind models to bipolar outflows, and Königl (1989) investigated how the wind might smoothly join a pattern of accretion flow inside the disk. Heyvaerts and Norman (1989) studied how the winds might collimate asymptotically into jets, while Uchida & Shibata (1985) and Lovelace et al. (1991) advocated alternative driving mechanisms where magnetic pressure gradients play a bigger role in the acceleration of a disk-blown wind.

Motivated by the problem of binary X-ray sources, a parallel line of research developed concerning how magnetized stars accrete from surrounding disks. Ghosh & Lamb (1978) used order-of-magnitude arguments to show that a strongly magnetized star would truncate the surrounding accretion disk at a larger radius than the stellar radius R_* and divert the equatorial flow along closed field-line funnels toward the polar caps. Although Ghosh and Lamb thought that this inflow would spin up the central object faster than if the accretion disk had extended right up to the stellar surface, Königl (1991) made the surprising and insightful suggestion that the process might torque down the star and account for the relatively slow rate of spin of observed T Tauri stars. Observational support for magnetospheric braking and accretion was subsequently marshalled by Edwards et al. (1993) and Hartmann et al. (1994).

Arons, McKee, and Pudritz (Arons 1986) proposed that a centrifugally-driven outflow accompanies the funnel inflow [see also Camenzind (1990)]. Independently, Basri (1989, unpublished) arrived observationally at the same suggestion by extending the synthesis work by Bertout et al. (1988) on ultraviolet excesses in T Tauri stars (for a review, see Bertout 1989). Shu et al. (1994a) put these ideas together into a concrete proposal that generalized the earlier X-wind model of Shu et al. (1988). Shu et al. (1995) considered how X-winds asymptotically collimate into YSO jets.

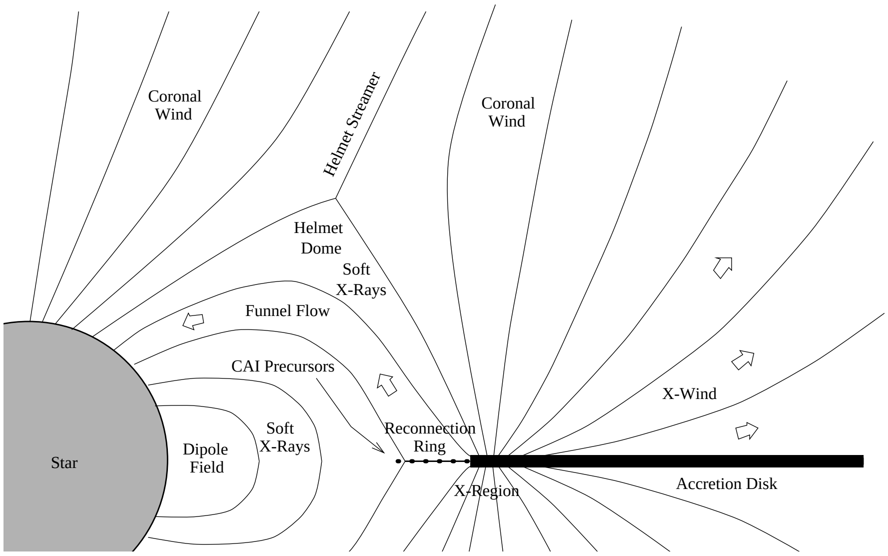

Figure 8. Schematic drawing of the X-wind model. Coronal winds from the star and the disk may help the X-wind to open field lines surrounding the helmet streamer, but this aspect of the configuration is not central to the model.

12. Generalized X-wind Model

In the generalized X-wind model, if the star has mass M_* and magnetic dipole moment μ_*, the gas disk is truncated at an inner radius,

$$R_{\rm x} = \Phi_{\rm dx}^{-4/7}\left(\frac{\mu_*^4}{GM_*\dot{M}_D^2}\right)^{1/7}. \tag{21}$$

A disk of solids may extend inward of $R_{\rm x}$ to the evaporation radius of calcium-aluminum silicates and oxides [see Shang et al. (1997) and Meyer et al. (1997)]. In equation (21), $\Phi_{\rm dx}$ is a dimensionless number of order unity that measures the amount of magnetic dipole flux that has been pushed by the disk accretion flow to the inner edge of the disk. In the closed dead-zone model of Najita & Shu (1994) and Ostriker & Shu (1995), $\Phi_{\rm dx} = 2\bar{\beta}_{\rm w} f^{1/2}$, with $f = \dot{M}_{\rm w}/\dot{M}_D$ and $\bar{\beta}_{\rm w}$ defined as the streamline-averaged ratio of magnetic field to wind mass-flux. This expression for the coefficient $\Phi_{\rm dx}$ holds when magnetic flux is swept toward $R_{\rm x}$ from both larger and smaller radii (see below), and the magnetic flux trapped in a small neighborhood of $R_{\rm x}$ is 3/2 times larger than the pure dipole value.

For a Keplerian disk, the inner edge of the disk rotates at angular speed

$$\Omega_{\rm x} = \left(\frac{GM_*}{R_{\rm x}^3}\right)^{1/2}. \tag{22}$$

To satisfy mass and angular momentum balance, the disk accretion divides at R_x into a wind fraction, $\dot{M}_\mathrm{w} = f\dot{M}_D$, and a funnel-flow fraction, $\dot{M}_* = (1-f)\dot{M}_D$, where

$$f = \frac{1 - \bar{J}_* - \tau}{\bar{J}_\mathrm{w} - \bar{J}_*}. \tag{23}$$

In equation (23) $\bar{J}_*$ and $\bar{J}_\mathrm{w}$ are, respectively, specific angular momenta nondimensionalized in units of $R_\mathrm{x}^2\Omega_\mathrm{x}$ and averaged over funnel and wind streamlines, and τ is the negative of the viscous torque of the disk, $-\mathcal{T}$, acting on its inner edge and measured in units of $\dot{M}_D R_\mathrm{x}^2\Omega_\mathrm{x}$. In the approximation that the embedded stellar fields force the X-region to be only weakly differentially rotating (Shu et al. 1994a,b), τ is small compared to unity. Similarly, if the funnel flow does not bring so much angular momentum into the (small) star as to spin it up on a time scale much shorter than the time to accumulate the star, $\bar{J}_*$ must also be negligible in comparison to unity.

In steady state, the star is regulated to corotate with the inner disk edge,

$$\Omega_* = \Omega_\mathrm{x}. \tag{24}$$

If corotation did not hold, the system would react to reduce the discrepancy between Ω_* and Ω_x, where Ω_x is given by equation (22) with R_x determined by how much magnetic field there is to maintain a certain average standoff distance for the stellar magnetosphere [see eq. (21)]. For example, suppose the star turns faster than the inner edge of the disk, $\Omega_* > \Omega_\mathrm{x}$. The field lines attached to both would then continuously wrap into ever tighter trailing spirals, with the field lines adjacent to the star tugging it backward in the sense of rotation. This tug decreases the star's angular rate of rotation Ω_* to more nearly equal the rate Ω_x. Conversely, imagine that $\Omega_* < \Omega_\mathrm{x}$. With the star turning slower than the inner edge of the disk, the field lines attached to both would continuously wrap into ever tighter leading spirals, with the field lines adjacent to the star tugging it forward in the sense of rotation. This tug increases the star's angular rate of rotation Ω_*, again to more nearly equal the rate Ω_x. In true steady state, $\Omega_* = \Omega_\mathrm{x}$, and the funnel-flow field lines acquire just enough of a trailing spiral pattern (but without continuously wrapping up) so that the excess of material angular momentum brought toward the star by the inflowing gas is transferred outward by magnetic torques to the footpoints of the magnetic field in the disk (Shu et al. 1994a,b).

The X-wind gas gains angular momentum and the funnel gas loses angular momentum at the expense of the matter at the footpoint of the field in, respectively, the outer and inner parts of the X-region. As a consequence, this matter and the field lines across which it is diffusing pinch toward the middle of the X-region. In an idealized treatment, where the pinch is imagined to gather the trapped flux into a narrow ring (a single point in the meridional plane), 1/3 of the trapped flux yields field lines pointing in the right outward directions to launch a (cold) X-wind; another 1/3 are pointing in the right inward directions to torque down the inflowing gas into a funnel flow; and the middle 1/3 are standing too upright to induce dynamical imbalance and result in a dead zone (Ostriker & Shu 1995). We assume that the Balbus & Hawley (1992) instability occurs inside the disk on dead zone field lines. The instability allows gas near the midplane to transfer from the last of the X-wind field lines to the first of the funnel-flow field lines. Thus, of the totality of field lines in the X-region, 1/3 yield outflow via the X-wind, and 2/3 yield inflow either via the Balbus-Hawley instability or via the funnel flow. On the assumption that incoming matter from the outer disk are loaded onto the tangle of field lines in the X-region more or less randomly, we may then deduce that $\dot{M}_{\rm w} \approx \dot{M}_D/3$, i.e., that $f \approx 1/3$.

If we adopt the approximations $\bar{J}_* \approx 0$ and $\tau \approx 0$ in equation (23), the condition $f \approx 1/3$ yields $\bar{J}_{\rm w} \approx 3$ (which requires for self-consistency a field-to-wind-flux loading $\bar{\beta}_{\rm w} \approx 1$). When X-wind field lines are loaded by disk accretion so that the magnetocentrifugal fling yields an average dimensionless wind torque $\bar{J}_{\rm w}$, the formula for the terminal speed of the X-wind (averaged over streamlines) reads

$$\bar{v}_{\rm w} = \left(2\bar{J}_{\rm w} - 3\right)^{1/2} \Omega_{\rm x} R_{\rm x}. \tag{25}$$

With $\bar{J}_{\rm w} \approx 3$, equation (25) becomes $\bar{v}_{\rm w} \approx \sqrt{3}\Omega_{\rm x} R_{\rm x}$, which gives $\bar{v}_{\rm w} \approx 200$ km s^{-1} for typical estimates of the Keplerian velocity $\Omega_{\rm x} R_{\rm x}$ at the inner edges of YSO accretion disks.

Shu et al. (1997) point out that the idealized steady state of exact corotation probably cannot be maintained because of dissipative effects. Two surfaces of null poloidal field lines – labeled as "helmet streamer" and "reconnection ring" in Figure 8 – mediate the topological behavior of dipole-like field lines of the star, opened field lines of the X-wind, and trapped field lines of the funnel inflow emanating from the X-region. Across each null surface, which begin or end on "Y-points" [called "kink points" by Ostriker & Shu (1995)], the poloidal magnetic field suffers a sharp reversal of direction. By Ampére's law, large electric currents must flow out of the plane of the Figure along the null surfaces. Nonzero electrical resistivity would lead to the dissipation of these currents and to the reconnection of the oppositely directed field lines [see, e.g., Biskamp (1993)].

Thus, we anticipate that realistic YSO systems will alternate between states where the magnetic field lines of the dead zone are open (see Fig. 8) and states where they are closed (see Fig. 9). The release of magnetic energy in transforming one state to another in giant flares presumably

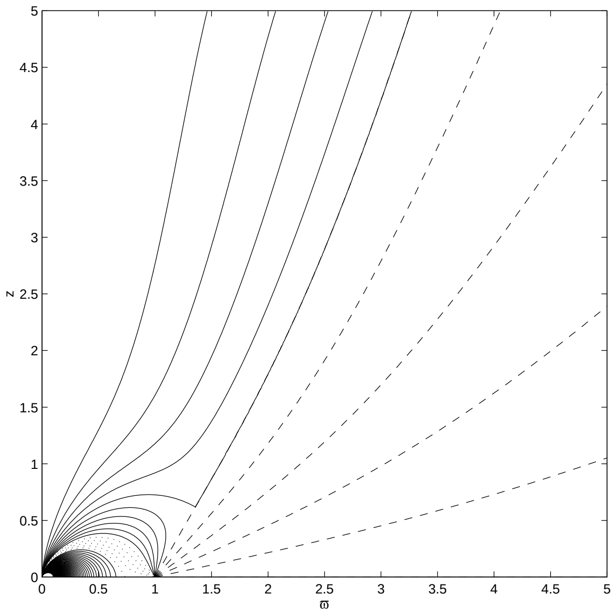

Figure 9. The poloidal magnetic field configuration resulting from the interaction of a magnetized star and a surrounding accretion disk. This Figure differs from Figure 8 in two respects. First, the dead zone is closed rather than open. Second, the field lines are not drawn schematically but result from an actual self-consistent calculation (Ostriker, Shang, and Shu, unpublished) that imposes approximate pressure balance across the interfaces of the funnel flow (dotted curves), dead zone (solid curves), and X-wind (dashed curves). Also denoted by solid curves are stellar field lines opened by the X-wind (i.e., those that connect at infinity to the dashed lines in the X-wind) and virtually unperturbed dipole field lines that are rooted in the star.

underlies a part of what observers call the "magnetic activity" of YSOs (e.g., Montmerle & André 1988; Feigelson, Carkner, & Wilking 1998). The change in magnetic topology will modify the numerical value of the coefficient Φ_{dx} in equation (21).

When R_{x} changes, the angular speed Ω_{x} of the footpoint of magnetic field lines in the X-region will vary according to equation (22). However, the considerable inertia of the star prevents its angular velocity Ω_* from changing on the time scale of magnetic reconnection at the null surfaces of the magnetosphere. The resultant shear when $\Omega_* \neq \Omega_{\mathrm{x}}$ will stretch and amplify field lines attached to both the star and the disk. The poloidal field will bulge outward from the increased magnetic pressure, inserting more magnetic flux into the fan of field lines emanating from the X-region [see the simulations of Linker & Mikić (1994) and Hayashi, Shibata, & Matsumoto (1996)]. Dynamo action inside the star would presumably replace the upward rising dipole-like poloidal fields. This dynamo action would be enhanced by the wrapping of field lines between the star and disk. Averaged over long times, we envisage a secular balance, with enough dynamo-generated poloidal field being inserted into the X-region to balance the rate of field dissipation at the null surfaces.

13. Summary

We conclude with a summary. Giant molecular clouds are supported against their self-gravity in part by magnetic fields and in part by MHD turbulence. Because of nonlinear mode coupling, the decay of MHD turbulence occurs more quickly than had been previously suspected. In the absence of offsetting effects, this decay will produce highly flattened clouds. However, if the dimensionless mass-to-flux ratio is subcritical or marginally critical, $\lambda \leq 1$, the material is stable to global and local gravitational collapse. In isolated regions of star formation, ambipolar diffusion in dense cores is a process that can increase the local value of λ beyond the critical value of unity. In more crowded environments, the collisional agglomeration of cloud clumps in the direction of the mean field (which increases the mass M without increasing the flux Φ) is another process that can lead to supercritical cores.

In regions where $\lambda > 1$, the decay of turbulence can by itself lead to the formation of dense pivotal cores and the birth of stars. The inner regions of pivotal cores formed either by slow ambipolar diffusion or by faster turbulent decay are likely to assume power-law forms. The gravitational collapse of such pivotal states occurs in a self-similar fashion, from inside-out, and has no tendency to want to stop unless the region either runs out of matter (in which case the star-formation process is highly efficient), or the inflow is truncated (say, by the onset and development of a bipolar outflow). Bipolar outflows that occur in flattened sheets can produce many cloud cores strung out in long filaments. In critical or subcritical regions, the existence of such cores and filaments is not a signpost for overall gravitational collapse and hierarchical fragmentation. Rather, it simply attests to the power that YSO outflows (and other energetic events) have for sculpting the shapes and forms of molecular clouds, especially in regions of high-mass star formation (cf. Wiseman & Ho 1998).

In contrast with regions like the Taurus molecular cloud, which yield only the dispersed mode of star formation, large regions within molecular clouds which are (or become) magnetically supercritical probably give the clustered mode of star formation (Shu, Adams, & Lizano 1987, C. Lada and E. Lada, this volume). The efficiency of star formation is high in such regions, and the competition for matter among YSOs with different "feeding zones" may be the determinant process that fixes the masses of stars rather than outflows (e.g., Larson 1995). However, outflows may still play an important role (e.g., in setting the level of turbulence of such regions), although confusion limits the ability of observers to investigate such issues in crowded environments. The importance of stellar feedback for star formation in the clustered mode remains a challenge for any comprehensive theory of the birth of stars from giant molecular clouds.

Acknowledgements: This research is funded in part by a grant from the National Science Foundation and by the NASA Astrophysics Theory Program that supports a joint Center for Star Formation Studies at NASA/Ames Research Center, the University of California at Berkeley, and the University of California at Santa Cruz. The research of ECO is supported by NAG 53840.

References

Akeson, R. L., & Carlstrom, J. E. 1997, ApJ, 491, 254
Allen, A., & Shu, F. H. 1999a, ApJ, in preparation
Allen, A., & Shu, F. H. 1999b, ApJ, in preparation
Arons, J. 1986, in Plasma Penetration into Magnetospheres, ed. N. Kylafis, J. Papamastorakis, and J. Ventura (Iraklion: Crete Univ. Press), 115
Arons, J., & Max, C. E. 1975, ApJ, 196, L77
Balbus, S. A., & Hawley, J. F. 1992, ApJ, 400, 610
Bally, J., & Lada, C. J. 1983, ApJ, 265, 824
Basu, S. 1997, ApJ, 485, 240
Basu, S., & Mouschovias 1994, ApJ, 432, 720
Bertoldi, F., & McKee, C. F. 1992, ApJ, 395, 140
Bertout, C. 1989, ARAA, 27, 351
Bertout, C., Basri, G., & Bouvier, J. 1988, ApJ, 330, 350
Biskamp, D. 1993, Nonlinear Magnetohydrodynamics (Cambridge University Press)
Blandford, R. D., & Payne, D. G. 1982 MNRAS, 199, 883
Bodenheimer, P. 1980, in Fund. Prob. in Theory of Stellar Evol., IAU Symp. No. 93, ed. D. Sugimoto, D. Q. Lamb, D. N. Schramm (Dordrecht: Reidel), p. 5
Bonnor, W. B. 1956, MNRAS, 116, 351
Boss, A. 1999, in Protostars & Planets IV, ed. V. Mannings, S. Russell, & A. Boss (Tucson: Univ. Arizona Press), in press
Camenzind, M. 1990, in Reviews in Modern Astronomy 3, ed. G. Klare (Berlin: Springer), 259
Chandrasekhar, S. 1939, Stellar Structure (New York: Dover)
Ciolek, G. E., Königl, A. 1998, ApJ, 504, 257
Cohn, H. 1980, ApJ, 242, 765
Crutcher, R. M. 1999, ApJ, in press
Crutcher, R. M., Troland, T. H., Goodman, A. A., Heiles, C., Kazes, I., & Myers, P. C. 1993, ApJ, 407, 175
Cudworth, K. M., & Herbig, G. H. 1979, AJ, 84, 548
Ebert, R. 1955, Z. Ap., 37, 217
Edwards, S., Strom, S. E., Herbst, W., Attridge, J., Merrill, K. M., Probst, R., & Gatley, I. 1993, AJ, 106, 372.
Evans, N. J. 1999, ARAA, 37, in press
Feigelson, E. D., Carkner, L., & Wilking, B. A. 1998, ApJ, 494, L215
Fukui, Y., Sugitani, K., Takaba, H., Iwata, T., Mizuno, A., Ogawa, H., & Kawabata, K. 1986, ApJ, 311, L85

Galli, D., Lizano, S., Li, Z. Y., Adams, F. C., & Shu, F. H. 1999, ApJ, submitted
Galli, D., & Shu, F. H. 1993a, ApJ, 417, 220
Galli, D., & Shu, F. H. 1993b, ApJ, 417, 243
Gammie, C. F. & Ostriker, E. C. 1996, ApJ, 466, 814
Ghosh, P., & Lamb, F.K. 1978, ApJ, 223, L83
Goodman, A. A., Benson, P. J., Fuller, G. A., & Myers, P. C. 1993, ApJ, 406, 528
Hartmann, L., Hewitt, R., & Calvet, N. 1994, ApJ, 426, 669
Hartmann, L., & MacGregor, K.B. 1982, ApJ, 259, 180.
Hayashi, M. R., Shibata, K., & Matsumoto, R. 1996, ApJ, 468, L37
Heyvaerts, J., & Norman, C. 1989, ApJ, 347, 1055
Hoyle, F. 1953, ApJ, 118, 513
Hunter, C. 1962, ApJ, 135, 594
Klessen, R. S., Burkert, A., & Bate, M. R. 1998, ApJ, 501, L205
Königl, A. 1989, ApJ, 342, 208
Königl, A. 1991, ApJ, 370, L39
Lada, C. J. 1985, ARAA, 23, 267
Larson, R. B. 1995, MNRAS, 272, 213
Layzer, D. 1964, ARAA, 2, 341
Li, Z. Y. 1998a, ApJ, 493, 230
Li, Z. Y. 1998b, ApJ, 497, 850
Li, Z. Y., & McKee, C. F. 1996, ApJ, 464, 373
Li, Z. Y., & Shu, F. H. 1996, ApJ, 472, 211
Li, Z. Y., & Shu, F. H. 1997, ApJ, 475, 237
Linker, J. A., & Mikić, Z. 1994, ApJ, 430, 898
Lizano, S., & Shu, F. H. 1989, ApJ, 342, 834
Lovelace, R. V. E, Berk, H. L., & Contopoulos, J. 1991, ApJ, 379, 696
Lynden-Bell, D., & Eggleton, P. P. 1980, MNRAS, 191, 483
Lynden-Bell, D., & Wood, R. 1968, MNRAS. 138, 495
McLaughlin, D. E., & Pudritz, R. E. 1997, ApJ, 476, 750
MacLow, M. M., Klessen, R. S., Burkert, A., Smith, M. D., & Kessel, O. 1998, Phys.Rev.Lett. 80, 2754
McKee, C. F. 1989, ApJ, 345, 782
Mestel, L. 1965, QJRAS, 6, 161
Mestel, L. 1968, MNRAS, 138, 359
Mestel, L. 1985 in Protostars and Planets II, ed. D. C. Black & M. S. Matthews (Tucson: University of Arizona Press), p. 320
Mestel, L., & Spitzer, L. 1956, MNRAS, 116, 505
Mestel, L., & Strittmatter, P. A. 1967, MNRAS, 137, 95
Meyer, M. R., Calvet, N., & Hillenbrand, L. A. 1997, AJ, 114, 288
Mizuno, A., Onishi, T., Yonekura, Y., Nagahama, T, Ogawa, H., & Fukui, Y. 1995, ApJ, 445, L161
Mizuno, A., Onishi, T., Hayashi, M., Ohashi, N., Sunada, K., Hasegawa, T., & Fukui, Y. 1994, Nature, v. 368, no. 6473, 719
Montmerle, T., & André, P. 1988, in Formation and Evolution of Low-Mass Stars, ed. A. K. Dupree & M. T. V. Lago (Dordrecht: Kluwer), p. 225
Mouschovias, T. Ch., & Paleologou, E. V. 1980, ApJ, 237, 877
Mouschovias, T. Ch., & Spitzer, L. 1976, ApJ, 210, 326
Myers, P. C. 1995, in Molecular Clouds and Star Formation, ed. C. Yuan and J. H. You (Singapore: World Scientific), 47
Myers, P. C., & Benson, P. J. 1983, ApJ, 266, 309
Myers, P. C., & Fuller, G. A. 1993, ApJ, 402, 635
Myers, P. C., Ladd, E. F., & Fuller, G. A. 1991, ApJ, 372, L95
Myers, P. C., Fuller, G. A., Goodman, A. A., & Benson, P.J. 1991, ApJ, 376, 561
Myers, P. C., Lazarian, A. 1998, ApJ, 507, L157
Nagai, T., Inutsuka, S., & Miyama, S. 1998, ApJ, 506, 306

Najita, J.R., & Shu, F.H. 1994, ApJ, 429, 808
Nakano, T. 1979, PASJ, 31, 697
Nakano, T. 1998, ApJ, 494, 587
Nakano, T., & Umebayashi, T. 1980, PASJ, 32, 613
Norman, C., & Silk, J. 1980, ApJ, 238, 158
Onishi, T., Mizuno, A., & Fukui, Y. 1999, PASJ Letter, in press
Onishi, T., Mizuno, A., Kawamura, A., Ogawa, H., & Fukui, Y. 1998, ApJ, 502, 296.
Ostriker, E.C., Gammie, C.F., & Stone, J.M. 1999, ApJ, in press
Ostriker, E.C., & Shu, F.H. 1995, ApJ, 447, 813
Padoan, P., & Nordlund, A. 1999, ApJ, submitted
Pudritz, R. E. 1986, PASP, 98, 709
Pudritz, R. E., & Norman, C. A. 1983, ApJ, 274, 677
Pudritz, R. E., & Norman, C. A. 1986, ApJ, 301, 571
Reipurth, B., Bally, J., & Devine, D. 1997, AJ, 114, 2708
Rodriguez, L. F., Ho, P. T. P., & Moran, J. M. 1980, ApJ, 240, L149
Schwarzschild, M. 1958, Structure and Evoultion of the Stars (Princeton University Press)
Shang, H., Shu, F., Lee, T., & Glassgold, A.E. 1997, in Low Mass Star Formation from Infall to Outflow, Poster Proc. IAU Symp. No. 182, ed. F. Malbet and A. Castets (Grenoble: Laboratorie d'Astrophysique), 312
Shu, F. H. 1977, ApJ, 214, 488
Shu, F. H. 1992, The Physics of Astrophysics, II. Gas Dynamics (Mill Valley: University Science Books)
Shu, F. H. 1995, in Molecular Clouds and Star Formation, ed. C. Yuan and J. H. You (Singapore: World Scientific), p. 97
Shu, F. H., Adams, F. C., & Lizano, S. 1987, ARAA, 25, 23
Shu, F. H., & Li, Z. Y. 1997, ApJ, 475, 251
Shu, F.H., Lizano, S., Ruden, S., & Najita, J. 1988, ApJ, 328, L19
Shu, F.H., Najita, J., Ostriker, E. C., & Shang, H. 1995, ApJ, 455, L155
Shu, F., Najita, J., Ostriker, E., Wilkin, F., Ruden, S., & Lizano, S. 1994a, ApJ, 429, 781
Shu, F. H., Najita, J., Ruden, S. P., & Lizano, S. 1994b, ApJ, 429, 797
Shu, F. H., Shang, H., Glassgold, A. E., & Lee, T. 1997, Science, 277, 1475
Shu, F. H., & Terebey, S. 1984, in Cool Stars, Stellar Systems, and the Sun, ed. S. Baliunas & L. Hartmann (Berlin: Springer-Verlag), p. 78
Spitzer, L. 1942, ApJ, 95, 329
Strittmatter, P. A. 1966, MNRAS, 132, 359
Stone, J. M., & Norman, M. L. 1992, ApJ Suppl, 80, 791
Stone, J. M, Ostriker, E. C., & Gammie, C. F. 1998, ApJ, 508, L99
Terebey, S., Shu, F. H., & Cassen, P. 1984, ApJ, 286, 529 (TSC)
Tohline, J. 1982, Fund. Cosmic Phys., 8, 1
Torrelles, J. M., Rodriguez, L. F., Canto, J., Carral, P., Marcaide, J., Moran, J. M., and Ho, P. T. P. 1983, ApJ 217, 214
Torrelles, J. M., Gomez, J. F. Ho, P. T. P., Rodriguez, L. F., Anglada, G., and Canto, J. 1994, ApJ, 435, 290
Uchida, Y., & Shibata, K. 1985, PASJ, 37, 515
Vrba, F. J., Strom, K. M., & Strom, S. E. 1976, AJ, 81, 958
Wardle, M., & Königl, A. 1993, ApJ, 410, 218
Welch, W. J., Vogel, S. N., Plambeck, R. L., Wright, M. C. H., & Bieging, J. H. 1985, Science, 228, 1329.
Wiseman, J., & Ho, P. T. P. 1998, ApJ, 502, 676
Yu, K. C., Bally, J., Devine, D. 1997, ApJ, 485, L45
Zuckerman, B., & Evans, N. J. 1974, ApJ, 192, L149